A Precast Concrete Roof Bracing System for Industrial Buildings

N.M. Angel
Doctoral Research Assistant, Universidad de los Andes, Colombia

H. Santa Maria & C. Lüders
Professor, Dept. of Structural Engineering, Pontificia Universidad Católica de Chile, Chile

SUMMARY:
The seismic behavior of a precast concrete roof bracing-system for industrial buildings composed by prestressed elements, known as Dalla-beams, and wet connections, is experimentally and analytically studied. Tests results show that the response of this wet connection is suitable for earthquake regions in terms of strength, ductility, energy dissipation capacity, and stiffness. The analytical phase of this investigation aimed to simulate the observed experimental behavior through bond-slip models for reinforcement bars embedded in concrete and degrading stiffness hysteretic models, obtaining satisfactory results. Recommendations to model the connection are given. Finally, earthquake performance of the tested brace system was adequate, showing small number of moderate damage, which provided information to improve the detailing of the connection.

Keywords: Cast-in-place joint; diaphragm; industrial structures; prestressed concrete; roof bracing system.

1. INTRODUCTION

Chile is worldwide known as a country of high seismic risk due to its proximity to the subduction zone between Nazca and South American plates. The strongest earthquake ever recorded hit the mid south Chile in 1960 and lately, on February 27th 2010, an Mw 8.8 earthquake occurred near Concepcion, Chile´s second largest city. Several large industrial facilities are based in that area, and many of them consist of reinforced/precast concrete structures using cantilever columns as seismic resistant system. The lack of redundancy and diaphragm effect on structures in high seismic zones -i.e. cantilever columns and pin connected structures- leads to unsuitable structural behavior and often the collapse of the structures. Column-beam joints are the most brittle point when the seismic resistant system is provided only through frames. Current design codes, like ACI 318, establishes conservative provisions for precast concrete frame structures in high seismic zones, resulting in considerable construction expenses (Khaloo A and Parastesh H., 2003).

According to Mizam and Kiran (2009), about 80% of industrial buildings in Turkey are precast concrete structures and 90% of them are located in high seismic zones. Kaplan et al. (2009) have studied Turkish practice in the construction of industrial buildings (pin connected precast concrete structures), that performed poorly during the Ceyhan and Marmara earthquakes. Gosh and Cleland (2012) reported that, with the exception of the out-of-date gable frame system, precast concrete systems performed well during the 2010 Chile earthquake. The Chilean code for seismic design of industrial buildings (INN, 2003) establishes that in buildings with cantilever columns used as the seismic resistant system, a roof bracing-system able to transfer horizontal loads and to provide structural redundancy has to be provided. Such bracing-system can be designed with diagonal steel elements axially loaded, or with an alternative system able to perform as a diaphragm. In this research, a roof bracing-system composed of prestressed concrete elements, known as Dalla-beams, and wet connections is studied. The analytical and experimental behavior of this bracing system is analyzed. Linear and nonlinear analyses of three types of tests on the wet connection are performed in order to validate the proposed roof bracing system for industrial buildings.

2. DESCRIPTION OF THE STUDIED ROOF BRACING SYSTEM

Dalla-beams are thin U-shaped prestressed concrete elements that are intended to act as seismic bracing system and roof support. They are 1145 mm wide at the top, while the bottom is 535 mm wide, with a maximum height of 297 mm and an average thickness of 40 mm (see Fig. 2.1). In order to achieve large spans, the Dalla-beams are prestressed through ϕ5mm wires and reinforced with welded wire mesh, with yield strength of 490MPa. Concrete compression strength is 35MPa.

The Dalla-beams are connected to the main beams of the frames through a cast in place 900x400x150mm block–wet joint, made of high strength mortar with compression strength of 80MPa, and two ϕ16mm hair-pin steel bars with a 180-degree hook, embedded into the joint, emulating a monolithic connection. Nominal yield strength of the ϕ16mm hair-pin steel bars is 420MPa. The prestressed wires emerging from the Dalla-beam are cast into the wet joint without any tensile stress in this zone. The configuration of the Dalla-beams as roof bracing system emulates the behavior of a horizontal Vierendeel truss, able to transfer horizontal bending due to seismic actions through the wet-joints at both of its ends. The configuration details of the Dalla-beams and the connection, as well as an illustration of the construction of an industrial building with Dalla-beams as roof bracing system are shown in Fig. 2.1.

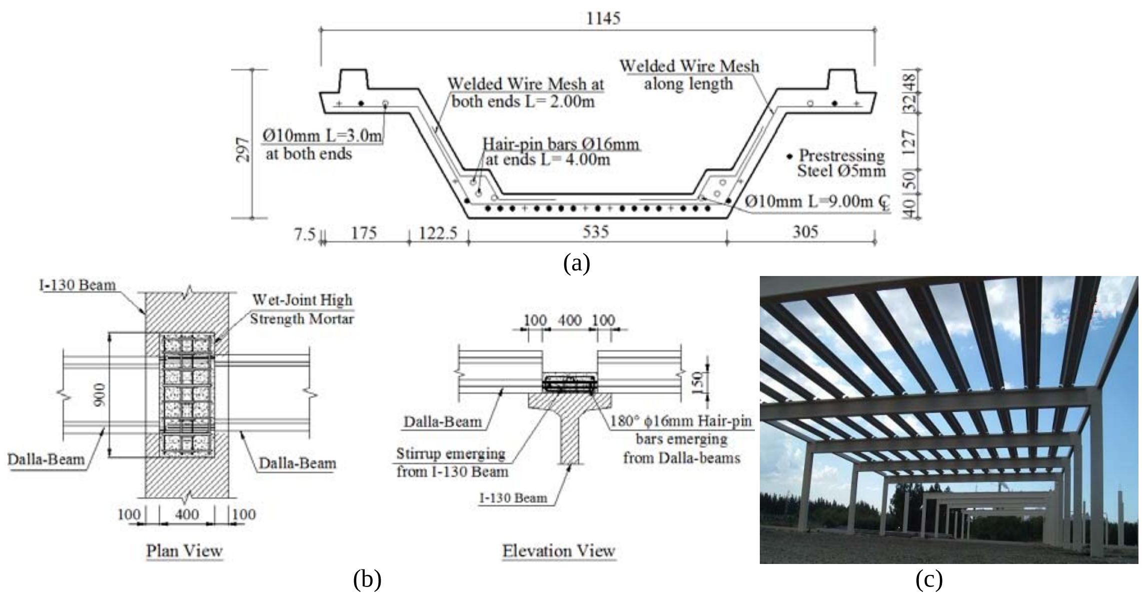

Figure 2.1. Dalla-beam section details; (b) wet joint block dimensions and details; and (c) construction of an industrial building with Dalla-beams. Beam notation from Preansa S.A. (Dimensions in mm)

3. EXPERIMENTAL PROGRAM

The experimental program consisted of three types of tests: monotonic tension loading tests of the 16-mm bars embedded into the Dalla-beams; monotonic tension loading tests of the 16-mm bars embedded into the cast in place connections; and cyclic loading tests of the full connection in accordance with a prescribed displacement history.

3.1. Monotonic tension loading tests of bars embedded into the Dalla-beams (LTBED)

These tests were made to understand the behavior and strength of the anchorage of hair-pin bars into the Dalla-beams when they are subjected to monotonic tensile loads. Figure 3.1(a) shows the arrangement of the specimens used in these tension loading tests, while Figure 3.1(b) illustrates the typical failure mode observed during the tests. Five specimens were tested.

(a)

(b)

Figure 3.1. Monotonic tension loading tests of bars embedded into the Dalla-beams: (a) Arrangement; (b) Typical failure mode of Dalla-beams specimens provided by Preansa S.A.

The observed behavior of the specimens showed that the hair-pin bars developed strength beyond the nominal yield stress with high strain ductility. It was also observed high influence of bar slippage in the total deformation measured. Slippage occurred due to the spreading of cracks in the thin Dalla-beam, the spalling of concrete cover – splitting tensile failure occurred – and the failure of the welded wire mesh. The results obtained in these tests for the maximum applied load and measured relative displacements of the hair-pin bar with respect to the Dalla-beam specimen are given in Table 3.1. Response curves are discussed in Section 4.

Table 3.1. Results for each specimen at maximum load (LTBED)

TEST	**Maximum Load (kN)**	**Stress on Bars (MPa)**	**Relative Displacement (mm)**
LTBED -1	330	821	-
LTBED -2	305	760	31.0
LTBED -3	278	691	41.3
LTBED -4	278	691	30.2
LTBED -5	257	640	76.8
Average	289.7	720.6	44.8
Standard Deviation	28.3	705.0	21.9
CV	0.098	0.098	0.49

3.2. Monotonic tension loading tests of bars embedded into the wet joint (LTBEW)

The hair-pin bars embedded into the wet joint were tested to measure their strength and behavior when a monotonic static load is applied at one side of the wet joint. The bar at the other side was anchored to the reaction frame. Four specimens were tested as shown schematically in Figure 3.2(a), while Figure 3.2(b) illustrates the typical crack pattern observed on top of the wet joint during the tests.

As in the previous test, the hair-pin bars developed strength beyond their nominal yield stress, with high strain ductility, but in this case no bar slippage was observed. In all LTBEW tests, the failure mode occurred by rupture of the loaded hair pin bar. At this point, minor local cracks on the wet joint concrete were observed (see Fig. 3.2(b)). The results obtained in these tests for the maximum applied load are given in Table 3.2. Response curves are discussed in Section 4.

3.3. Cyclic loading tests (CLT)

Two Dalla-beams joined to an I-130 beam through a wet connection were tested within a reaction frame, applying increasing cyclic lateral load up to failure. The linear and non linear features of the connection, as well as the hysteretic behavior, lateral stiffness degradation, energy dissipation, equivalent viscous damping, and the failure mode of the joint system were studied. Each specimen consisted of a Dalla-beam section, 2680 mm long, joined to an I-130 beam through the wet connection under study. The Dalla-beam section was arranged as a vertical cantilever horizontally loaded at 2380 mm from the connection. Displacement transducers were used to measure the horizontal displacement at 2100 mm from the connection. The test setup and the loading history are shown in Figure 3.3.

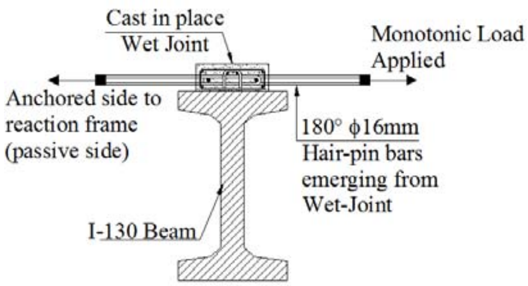

(a)

(b)

Figure 3.2. LTBEW Test: (a) Arrangement; (b) Crack pattern of top of the Wet-Joint

Table 3.2. Results for each specimen at maximum load (LTBEW)

Test	Maximum Load (kN)	Stress on Bars (MPa)	Relative Displacement Loaded Side (mm)	Relative Displacement Passive Side (mm)	Average Relative Displacement (mm)
LTBEW 1	233	580	12.0	3.6	7.8
LTBEW 2	272	677	20.0	17.7	18.9
LTBEW 3	267	663	12.5	20.3	16.4
LTBEW 4	281	698	28.0	-	28.0
Average	263	655	18.1	13.9	17.8
Standard deviation	207	515	7.5	9.0	8.3
CV	0.079	0.079	0.42	0.65	0.47

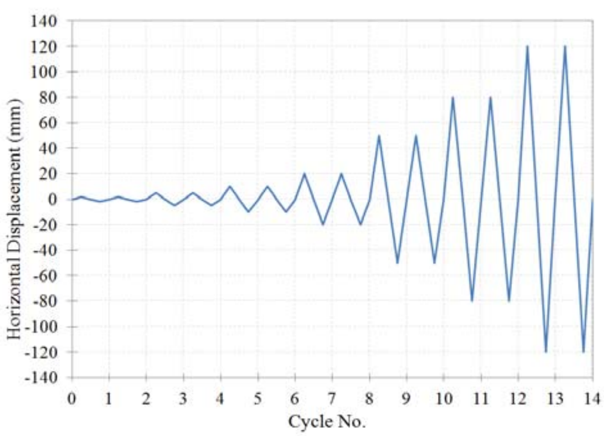

(a)

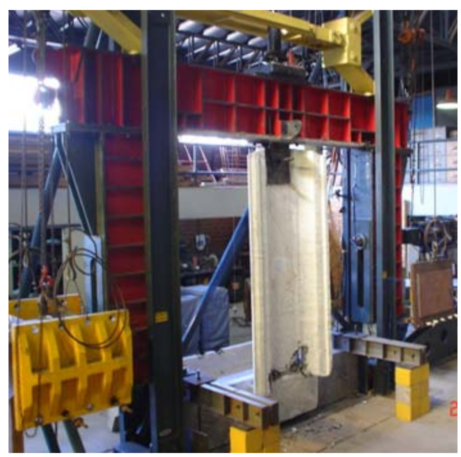

(b)

Figure 3.3. Cyclic loading tests (CLT): (a) Loading history; (b) Test setup

The hysteresis curves measured during the tests and the backbone curves for each test are plotted in Figure 3.4. Both tests showed similar hysteretic response: there is a large initial stiffness, up to yielding. The unloading branches of the curve maintain a large stiffness, even for large displacements, but the reloading occurs with an important decrease of the stiffness as the displacements increase. After yielding, it can be observed a slight decrease of strength within cycles. There is an important ductility in the wet connection, without significant strength degradation, and high capacity on the basis of stiffness and strength until 80mm displacement. Since the horizontal displacements were measured

2100mm above the connection, 80mm displacement is equivalent to 0.038 radians rotation. Beyond this point, it was observed pinching of the hysteresis loops, when the hair pin bars were responsible of the system's stiffness.

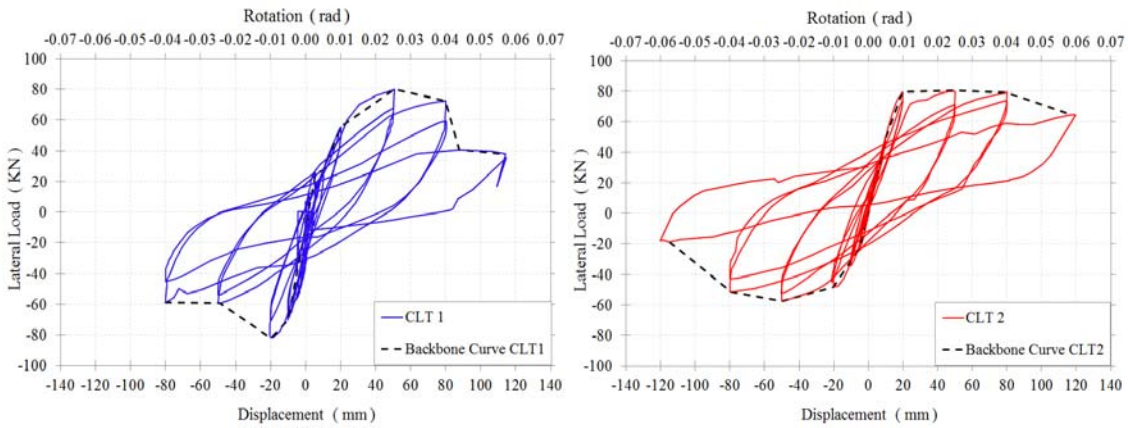

(a) (b)

Figure 3.4. Hysteresis and backbone curves of the hysteresis loops (a) CLT 1 and (b) CLT 2

The failure of the specimens was considered at the point in which the applied load could not be increased beyond 80% of the maximum measured lateral load. At that load level the displacement ductility is about 4.66. Beyond this point, there is important strength and stiffness degradation during loading, while in the unloading branches the stiffness remains fairly constant. This phenomenon may be explained by the loss of bond of the 16-mm hair pin bars, which can be observed in the cumulative damage of the concrete on the Dalla-beam, as shown in Figure 3.5. This damage occurred due to the very small concrete cover and the absence of transverse reinforcement around the 16-mm hair pin bars. Only small cracks were observed on the I-130 beam. From the tests results, it can be inferred that there is certain flexibility on the connection zone because of the hair pin bars slippage from their embedment into the Dalla-beam.

Figure 3.5. Cumulative damage of the concrete during cyclic loading tests (CLT)

4. EVALUATION OF THE EXPERIMENTAL RESULTS

Bond-slip models proposed by Alsiwat and Saatcioglu (1992) and by Sezen (2002) were used to emulate the empirical observations of the Monotonic Tension Loading Tests of Bars Embedded into the Dalla-beams (LTBED) and Monotonic Tension Loading Tests of Bars Embedded into the Wet Joint (LTBEW). Experimental material properties such as concrete compression strength f'_c, steel yielding (f_y) and ultimate strengths (f_u), modulus of elasticity of the steel E_s, and strains at yield point (ε_y), strain hardening (ε_{sh}) and at ultimate strength (ε_u) of the steel, used in the calculation of the bond-slip models, are given in Table 4.1. Comparisons between experimental results and analytical models are presented in Fig. 4.1.

Table 4.1. Material properties for the bond-slip models

f'_c (MPa)	f_y (MPa)	f_u (MPa)	E_s (MPa)	ε_y	ε_{sh}	ε_u
35	485	654	210000	0.00231	0.02	0.12

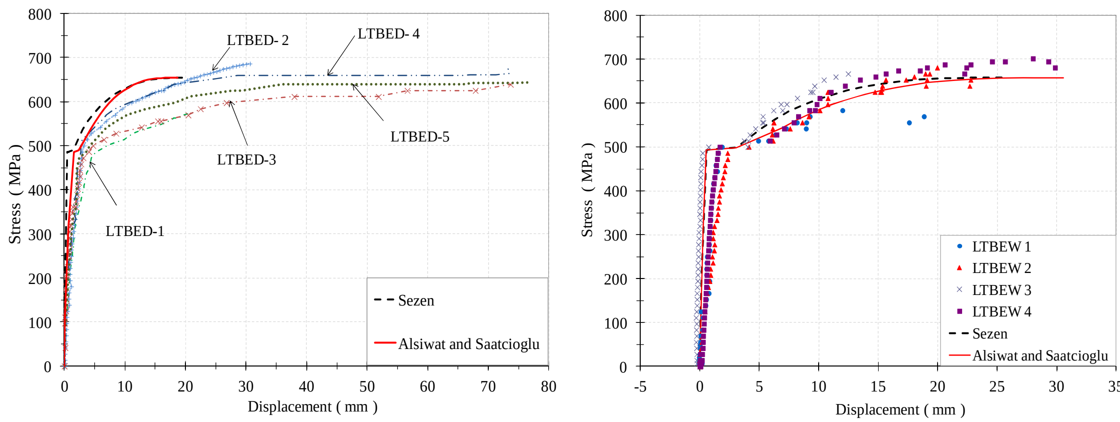

(a) (b)

Figure 4.1. Comparison between bond-slip models and tests results: (a) Bar embedded into Dalla-beams (LTBED; (b) Bar embedded into the wet joint (LTBEW)

It can be seen in Fig 4.1(a) that the analytical models underestimate the deformations measured in the LTBED tests by up to 70%. This may be because most of the deformation measured during these tests occurred due to large slip of the 16-mm bars embedded in the Dalla-beams, due to the small concrete cover and absence of confinement reinforcement of the 16-mm bars within the Dalla. Deformations calculated using analytical models by Alsiwat and Saatcioglu (1992), and Sezen (2002) are 64% and 85%, respectively, smaller than the average deformations at yield point measured in the tests of the bars embedded into the Dalla-beams. It shows that bond stress between concrete and hair-pin bars is actually small, even at elastic range of behavior, and the slippage component of the deformations measured is large before yielding of the bars. This difference is not due to an inadequate embedment length but because of the small concrete cover that makes it impossible to reach the theoretical bond strength. On the other hand, in the case of the bars embedded into the cast in place connection, the analytical models reproduce very effectively the deformations observed during the test, particularly in the nonlinear (inelastic) range of behavior (Fig. 4.1(b)). The models also underestimate the strains before yield point, but differences between experimental and analytical results are smaller than those in the previous test. An appropriate concrete cover should result in a better bond performance and accuracy of the models when estimating the actual behavior.

5. MODELLING OF THE DALLA BEAM

Flexibility encountered on the joint due to slippage of the connecting bars requires an analytical model in which the Dalla-beam is connected to the I-130 beam through a spring with a finite rotational stiffness. Thus, the total horizontal displacement (δ) obtained from cyclic loading tests can be decomposed into displacement due to flexural response of the Dalla-beam (δ_f) and rotation at the connection because of the hair-pin bar slippage (δ_{slip}) (see Fig. 5.1), as given in Eqn. 5.1 and Eqn. 5.2 in terms of displacement and rotation respectively. The shear deformation is not considered because it is small compared with the others.

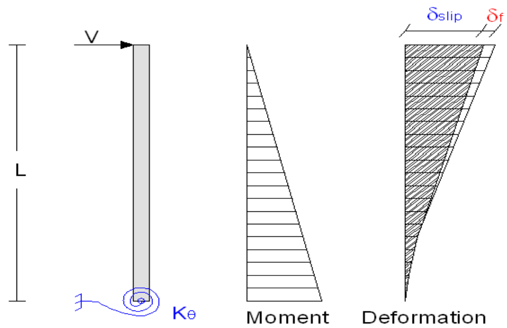

Figure 5.1. Distribution on height of moment and deformation

$$\delta = \delta_f + \delta_{slip} \tag{5.1}$$

$$\theta = \theta_f + \theta_{slip} \tag{5.2}$$

The flexural response of the Dalla-beam element is analyzed by separating the beam into two areas: i) the top length L-L_1, in which the response involves the complete cross-section of the Dalla-beam; and ii) a bottom length L_1, in which a smaller cross section is considered given that the actual connection involves contact between the joint and the Dalla-beam along a smaller part of the cross-section. The model shown in Fig. 5.2(a) was analyzed to evaluate the length L_1 by comparing the elastic lateral stiffness of a uniaxial model to results of finite elements models in SAP 2000 (Computers and structures Inc., 2006) (see Fig. 5.2(b)). Length L_2 is defined as the distance between L_1 and the point of measured displacements.

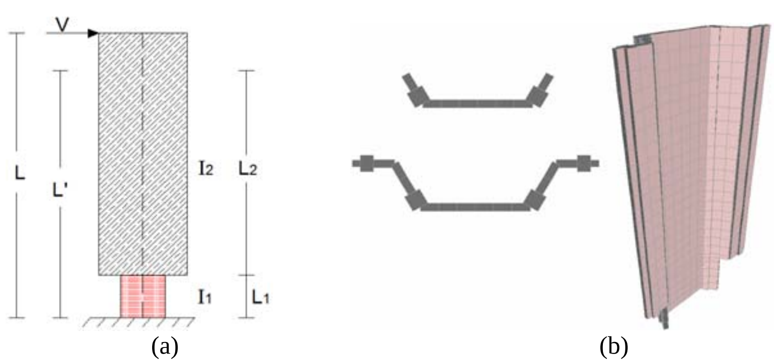

Figure 5.2. (a) Representation of the Dalla-beam section in height for the proposed model; (b) Finite element model analyzed

The elastic rotation at the end of the element due to flexural behavior of the Dalla-beam as modeled on Fig. 5.2(a) is given by Eqn.5.3:

$$\theta_f = \frac{M}{2EI_1 I_2 L}\left[I_1 L_2 (2L - L_1) + 2LL_1 (I_2 - I_1) - L_1^2 (I_2 - I_1)\right] \tag{5.3}$$

Where M is the moment at the base due to the lateral load, E is the concrete's modulus of elasticity, and I_1 and I_2 are the moments of inertia of the cross section in the direction of the lateral load, in the lengths L_1 and L_2 respectively. L_1 is taken equal to the plastic hinge length L_p proposed by Paulay and Priestley (1992). This plastic hinge length is approximately half the width of the Dalla-beam in contact with the cast-in place joint. The comparison with Finite Elements results showed that there is an overestimation of flexural rotation of less than 3%, small enough to accept the rotation calculated with Eqn. 5.3. On the other hand, the elastic rotational stiffness of the connection zone is given by Eqn. 5.4:

$$K_{\theta\, slip} = \frac{M}{\theta_{slip}} \tag{5.4}$$

Here θ_{slip} is the rotation in the connection zone due to slippage of the hair pin bar. This rotation is obtained analytically through Eqn. 5.5:

$$\theta_{slip} = \frac{\sum slip}{x} \tag{5.5}$$

Where Σslip is the sum of slippage of the hair-pin bars embedded into the cast in place connection and the Dalla-beam; and x is defined as the distance from the neutral axis to the centroid of the hair pin bar in tension. Both, Σslip and x should be calculated for the same stress level on the hair pin bar in tension. Σslip is reasonably represented by using the bond-slip model proposed by Alsiwat and Saatcioglu (1992) (see Fig. 4.1). Figure 5.3 shows the comparison between the rotational stiffness for the cracking moment calculated using the models proposed by Alsiwat and Saatcioglu (1992) and by Sezen (2002) according to Eqn. 5.4, and the stiffness calculated from the CLT tests. Results obtained using the bond-slip model given by Sezen (2002) are less accurate when compared with the measurements from cyclic loading tests. Therefore, the bond-slip model given by Alsiwat and Saatcioglu is used to calculate the elastic rotational stiffness of the connection.

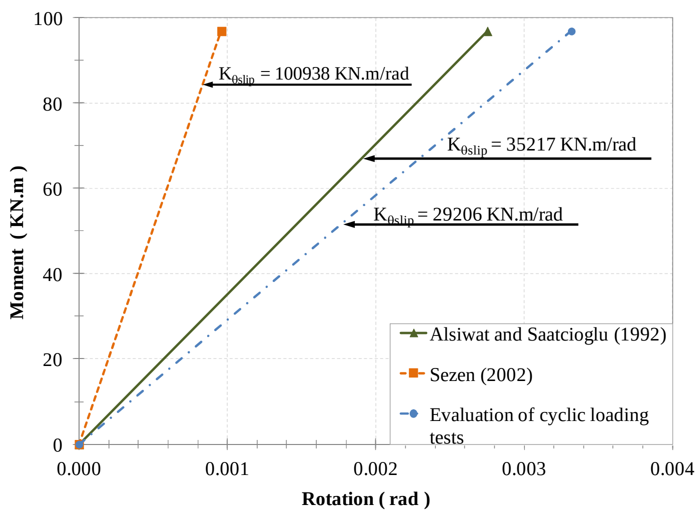

Figure 5.3. Rotational stiffness from analytical and tests evaluations

As was discussed before, deformations up to the yield point (within the range of elastic response) are separated into displacement due to flexural response of the Dalla-beam and rotation at the connection because of the hair-pin bar slippage. For deformations beyond this point, all the rotations of the Dalla-beam are considered to be due to the plastic curvature accumulated on the length L_1, so the total rotation in the inelastic range is computed as the sum of the rotation due to hair-pin bars slip for yield moment ($\theta_{slip\ yield}$) and the cumulative rotation due to plastic flexural behavior on the length L_1. This is not completely true, because there is a certain plastic bond-slip behavior, but it is not feasible to obtain from data tests and therefore, it is difficult to estimate in practice. Moreover, this assumption is conservative and reasonable for the model proposed. Thus, the plastic rotations are obtained from CLT test according to Eqn. 5.6:

$$\theta_p = \frac{\delta_p - \delta_y}{L' - \frac{L_1}{2}} \tag{5.6}$$

where δ_y and δ_p are the measured displacements at yield point and beyond the range of elastic response, respectively. The backbone curve moment-flexural rotation relationship is idealized as bilinear as per observation from the CLT tests, see Fig. 3.4(b), and for simplicity. Fig. 5.4(a) illustrates the backbone curve moment-flexural rotation obtained from Eqn. 5.5 and Eqn. 5.6, based on the measured response from CLT tests, and the idealized bilinear relationship proposed. The cyclic response of the bracing system connection under study was modeled with the Ruaumoko 2D (Carr, 2007) software, using the idealized moment-rotation relationship from Fig. 5.4(a), emulating the cyclic loading tests. The Modified Takeda model by Otani (1974) is used in order to reproduce the observed hysteretic features, incorporating stiffness degradation parameters (α=0 and β=0) during reloading and unloading respectively. Comparison between the analytical model and experimental results from CLT tests, in terms of hysteretic moment-rotation response, is plotted in Fig. 5.4(b).

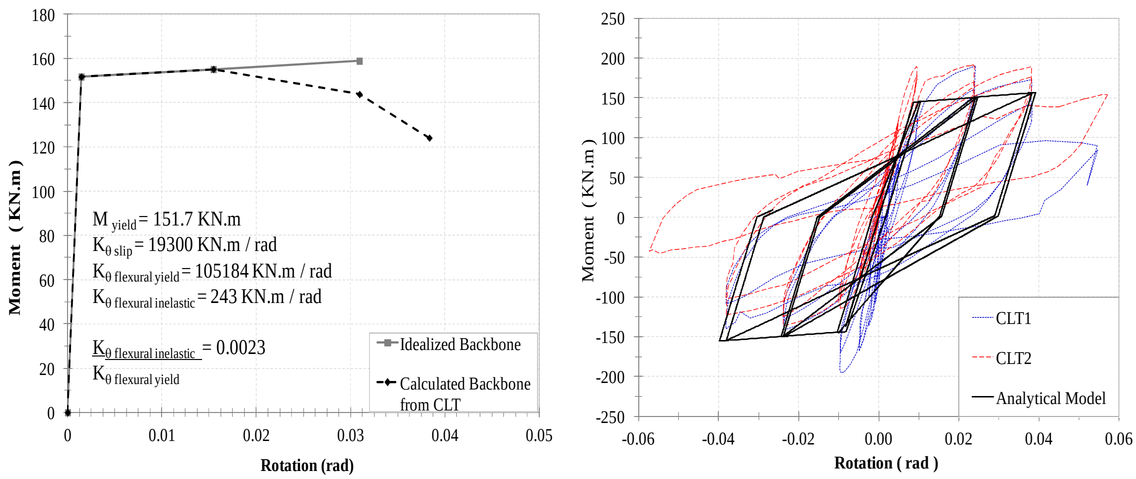

Figure 5.4. (a) Moment – flexural rotation backbone curve from CLT tests; (b) Measured hysteretic response and analytical hysteretic behavior

Hysteretic response modeled with Modified Takeda, taking into account the considerations explained above, correlates reasonably well with the actual response obtained from cyclic loading tests. Nevertheless, the response modeled with Modified Takeda does not predict accurately the experimental peak strength reached during tests, with a difference of up to 20%, and since it was adopted a bilinear moment-curvature backbone curve for model simplicity, the decay in strength and deformation capacity in the last loop are not captured by the model. However, the model response is considered conservatively accurate.

6. PERFORMANCE OF THE DALLA-BEAMS DURING THE FEBRUARY 27TH MAULE EARTHQUAKE

At the time of the earthquake 68250 m^2 of warehouses had been built using the Dalla-beam roof-bracing system. Cruz and Valdivia (2011) reported of a warehouse structured with prestressed beams supported on cantilevered columns, with a roof bracing system consisting of Dalla-beams with the wet connection described in here. Significant shaking occurred at the location of the warehouse, near Mininco, about 200 km south of the epicenter of the earthquake. Even though the contents of the warehouse were severely damaged, no damage was observed in the structural system, and no residual deflections occurred. Of the connections existing at the time of the earthquake, 0.34% suffered moderate damage, consisting of cracking of the mortar of the wet connection, cracking and spalling of the Dalla-beams at their support and cracking of the top beam that supports the Dalla-beams, near the wet connection. All the damage was moderate and easily reparable.

7. CONCLUSIONS

A precast concrete roof bracing-system for industrial buildings was experimentally and analytically studied. Three types of tests were carried out to know the behavior of this system, focusing on the response of the wet joint that connects the bracing system to the structure. Similarly, analytical models were analyzed to predict the observed experimental behavior based on bond–slip theories and hysteresis models, in order to provide a tool to be used in developing recommendations for design engineers and recommendations to fulfill the requirements provided by the Chilean code NCh 2369 for seismic design of industrial buildings using Dalla-beams as roof bracing-system.

Experimental tests showed a high inelastic displacement (rotation) capacity of the system, without significant strength and stiffness degradation during the cyclic behavior, which is suitable in seismic structural performance. There is certain flexibility on the connection zone because of the hair-pin bars slippage when they are embedded into the Dalla-beam and lesser in the wet joint. This rotation flexibility should be considered when analyzing structures that use Dalla-beams as roof bracing system and it can be calculated through the bond-slip model proposed by Alsiwat and Saatcioglu (1992). It was also observed that the hysteretic behavior is well represented by the Modified Takeda Model (Otani, 1974).

AKCNOWLEDGEMENT

The authors express their gratitude to Prefabricados Andinos S.A (PREANSA) for conceiving the design of the roof bracing system and for providing the tests specimens for this research work. The tests were performed at the request of PREANSA by the student María Olga Faúndez in the Laboratory of Structural Engineering of the Department of Structural and Geotechnical Engineering of the Pontificia Universidad Catolica de Chile during 2006-2007. The test specimens were built at the PREANSA plant at TilTil, and later assembled at the Laboratory.

REFERENCES

Alsiwat, J.M. and Saatcioglu, M. (1992). Reinforcement anchorage slip under monotonic loading. *ASCE Journal of Structural Engineering*. **118:9**, 2421-2438.

American Concrete Institute (2008). Building Code Requirements for Structural Concrete and Commentary (ACI 318M-08). Farmington Hills, MI, USA.

Carr, A. (2007). Ruaumoko manual. Theory. Christchurch, New Zealand: University of Canterbury.

Computers & Structures, Inc. – CSI (2006). SAP2000. Berkeley, CA, USA. Computers & Structures, Inc.

Cruz, E. F. and Valdivia, D., (2011). Performance of industrial facilities in the Chilean earthquake of 27 February 2010. *Structural Design Tall Special Buildings*. **20,** 83–101.

Dictuc S.A. (2008). Comportamiento estructural de nudos Dalla-Viga I-130. Ensayos experimentales. Informe No 738760, Dictuc S.A. – Pontificia Universidad Catolica de Chile, Santiago, Chile.

Instituto Nacional de Normalización (2003). Diseño sísmico de estructuras e instalaciones industriales (NCH2369). Santiago, Chile.

Khaloo, A. and Parastesh, H. (2003). Cyclic loading response of simple moment-resisting precast concrete beam-column connection. *ACI Structural Journal*. **100:S46**, 440-445.

Kaplan, H., Nohutcu, H., Cetinkaya, N., Yilmaz, S., Gonen, H. and Atimtay, E. (2009) Seismic strengthening of pin-connected precast concrete structures with external shear walls and diaphragms. *PCI Journal*. **54:1**, 88-99.

Mizam, D. and Kiran, N. (2009). Analysis of seismic load to prefabricated connection. *Proceedings of World Academy of Science, Engineering and Technology*. **38,** 1353-1364.

Otani, S. (1974). Analysis of Reinforced Concrete Frame Structures. *ASCE Journal of the Structural Division*. **100**, 1433-1449.

Paulay, T. and Priestley, M.J.N. (1992). Seismic design of reinforced concrete and masonry buildings. John Wiley and Sons, New Jersey, USA.

Sezen, H. (2002). Seismic behavior and modeling of reinforced concrete buildings columns. Doctoral Dissertation, University of California, Berkeley, USA.

Takeda, T., Sozen, M.A. and Nielson, N.N. (1970). Reinforced concrete response to simulated earthquakes. *ASCE Journal of the Structural Division*. **96**, 2557-2573.